

Multiple phase transitions of the susceptible-infected-susceptible epidemic model on complex networks

Angélica S. Mata¹ and Silvio C. Ferreira¹

¹*Departamento de Física, Universidade Federal de Viçosa, 36570-000, Viçosa, MG, Brazil*

We show that the susceptible-infected-susceptible (SIS) epidemic dynamics running on the top of networks with a power law degree distribution can exhibit multiple phase transitions. Three main transitions, explained through distinct mean-field theories, are identified: A short-term epidemics concentrated around the most connected vertex; a long-term (globally stable) localized epidemics with a vanishing threshold; and an endemic phase occurring at a finite threshold. In particular, we show that the threshold recently predicted by Boguñá *et al.* [Phys. Rev. Lett. **11**, 068601 (2013)] involves a transition to a long-term but still localized epidemics. We show that the multiple transitions are related to the activations of distinct connected domains of the network.

PACS numbers: 89.75.Hc, 05.70.Jk, 05.10.Gg, 64.60.an

I. INTRODUCTION

Phase transitions involving equilibrium and non-equilibrium processes on the top of complex networks have begun drawing an increasing interest soon after the boom of network science at late 90's [1]. Percolation [2], epidemic spreading [3], and spin systems [4] are only a few examples of breakthrough in investigation of classical critical phenomena in complex networks. Absorbing state phase transitions [5] have become a paradigmatic issue in the interplay between nonequilibrium systems and complex networks [6], being the epidemic spreading a prominent example where high complexity emerges from very simple dynamical rules on heterogeneous substrates [3, 7–11].

The existence/absence of finite epidemic thresholds involving an endemic phase of the susceptible-infected-susceptible (SIS) model on the top of scale-free (SF) networks with a degree distribution $P(k) \sim k^{-\gamma}$, where γ is the degree exponent, has been target of a recent and intense investigation [7–12]. In the SIS epidemic model, individuals can be only in one of two states: infected or susceptible. Infected individuals become spontaneously healthy at rate 1 (this choice fixes the time scale), while the susceptible ones are infected at rate λn_i , where n_i is the number of infected contacts of a vertex i .

Distinct theoretical approaches were devised to determine an epidemic threshold λ_c of the SIS model separating an absorbing, disease-free state from an active phase [7–13]. The quenched mean-field (QMF) theory [13] explicitly includes the entire structure of the network through its adjacency matrix while the heterogeneous mean-field (HMF) theory [3] performs a coarse-graining of the network structure grouping vertices accordingly their degree. The HMF theory predicts a vanishing threshold for the SIS model for the range $2 < \gamma \leq 3$ while a finite threshold is expected for $\gamma > 3$. Conversely, the QMF theory states a threshold inversely proportional to the largest eigenvalue of the adjacency matrix, implying that the threshold vanishes for any value of γ [7]. However, Goltsev *et al.* [8] proposed that QMF theory

predicts the threshold for an endemic phase, in which a finite fraction of the network is infected, only if the principal eigenvector of adjacency matrix is delocalized. In the case of a localized principal eigenvector, that usually happens for large random networks with $\gamma > 3$, the epidemic threshold is associated to the eigenvalue of the first delocalized eigenvector. For $\gamma < 3$, there exist a consensus for SIS thresholds: both HMF and QMF are equivalent and accurate for $\gamma < 2.5$ while only QMF works for $2.5 < \gamma < 3$ [9, 14].

Lee *et al.* [11] proposed that for a range $\lambda_c^{QMF} < \lambda < \lambda_c$ with a nonzero λ_c , the outliers (hubs) in a random network become infected but their activities are restricted to their neighborhoods. High-degree vertices produce independent active domains only when they are not directly connected. The sizes of these active domains increase for increasing λ leading to the overlap among them and, finally, to an endemic phase for $\lambda > \lambda_c$. However, on networks where almost all hubs are directly connected, it is possible to sustain an endemic state even in the limit $\lambda \rightarrow 0$ due to the mutual reinfection of connected hubs. Inspired in the appealing arguments of Lee *et al.* [11], Boguñá, Castellano and Pastor-Satorras (BCPS) [10] proposed a semi-analytical approach taking into account a long-range reinfection mechanism and again found a vanishing epidemic threshold for $\gamma > 3$. They compared their theoretical predictions with simulations starting from a single infected vertex and a diverging epidemic lifespan was used as a criterion to determine the thresholds. However, the applicability of BCPS theory to determine a phase transition involving an endemic phase has been debated [15].

In this work, we show that the SIS dynamics running on the top of SF networks with $\gamma > 3$ can exhibit multiple phase transitions if the degree distribution presents large gaps. Moreover, we show that the vanishing threshold predicted by the BCPS theory [10] represents a long-term but still localized epidemics rather than an endemic state. Finally, our numerical results strongly indicate a transition to the endemic state occurring at a finite threshold, which is intriguingly well described by the classic and

simpler HMF theory [3].

We have organized our paper as follows: in Sec. II we present the quasistationary (QS) simulation method used in the work. Section III is devoted to describe the numerical results and in the Sec. IV we draw our concluding remarks. Finally, we confront the QS method with lifespan method proposed in Ref. [10] in Appendix A and show that the latter may not determine the endemic phase in systems with multiple phase transitions.

II. SIMULATION METHODS

We implement the SIS model using the standard simulation scheme [9]: At each time step, the number of infected nodes N_i and edges emanating from them N_k are computed and time is incremented by $dt = 1/(N_i + \lambda N_k)$. With probability $N_i/(N_i + \lambda N_k)$ one infected node is selected at random and becomes susceptible. With the complementary probability $\lambda N_k/(N_i + \lambda N_k)$ an infection attempt is performed in two steps: (i) A infected vertex j is selected with probability proportional to its degree. (ii) A nearest neighbor of j is selected with equal chance and, if susceptible, is infected. If the chosen neighbor is infected nothing happens and simulation runs to the next time step. The numbers of infected nodes and related links are updated accordingly, and the whole process is iterated.

The simulations were performed using the QS method [16, 17] that, to our knowledge, is the most robust approach to overcome the difficulties intrinsic to the simulations of finite systems with absorbing states, in which every time the system tries to visit an absorbing state it jumps to an active configuration previously visited during the simulation (a new initial condition). This approach is completely equivalent to the standard QS method where averages are performed only over samples that did not visit the absorbing state [16]. To implement the method, a list containing $M = 70$ configurations is stored and constantly updated. The updating is done by randomly picking up a stored configuration and replacing it by the current one with probability $p_r \Delta t$. We fixed $p_r \simeq 10^{-2}$ since no dependence on this parameters was detected for a wide range of simulation parameters. After a relaxation time t_r , the averages are computed over a time t_{av} .

The characteristic relaxation time is always short for epidemics on random networks due to very small average shortest path [18]. Typically, a QS state is reached $t > 10^4$ for the simulation parameters investigated. So, we used $t_r = 10^5$. The averaging time, on other hand, must be large enough to guaranty that epidemics over the whole network was suitably averaged. It means that very long times are required for very low QS density (subcritical phase in phase transition jargon) whereas relatively short times are sufficient for high density states. Since long times are computationally prohibitive for highly infected QS states, we used averaging times from 10^5 to 10^9 , being the larger the average time the smaller

the infection rate. Notice that the simulation time step becomes tiny for a very supercritical system (large number of infected vertices) and a huge number of configurations are visited during a time interval $\Delta t = 1$. It is important to notice that the QS method becomes expendable for a large part of our simulations since the system never visits the absorbing state for the considered simulation times.

Both equilibrium and non-equilibrium critical phenomena are hallmarked by simultaneous diverging correlation length and time which microscopically reflect divergence of the spatial and temporal fluctuations [5], respectively. Even tough a diverging correlation length has little sense on complex networks due to the small-world property [19] the diverging fluctuation concepts are still applicable. We used different criteria to determine the thresholds, relied on the fluctuations or singularities of the order parameters, as explained below.

The QS probability $\bar{P}(n)$, defined as the probability that the system has n occupied vertices in the QS regime, is computed during the averaging time and basic QS quantities, as lifespan and density of infected vertices, are derived from $\bar{P}(n)$ [16]. Thus, the threshold for finite networks can be determined using the modified susceptibility [9]

$$\chi \equiv \frac{\langle n^2 \rangle - \langle n \rangle^2}{\langle n \rangle} = \frac{N(\langle \rho^2 \rangle - \langle \rho \rangle^2)}{\langle \rho \rangle}, \quad (1)$$

that does exhibit a pronounced divergence at the transition point for SIS [9, 11, 14] and contact process [6, 20] models on networks. See Refs. [6, 9] for further discussion on χ . The choice of the alternative definition, Eq. (1), instead of the standard susceptibility $\tilde{\chi} = N(\langle \rho^2 \rangle - \langle \rho \rangle^2)$ [21] is due to the peculiarities of dynamical processes on the top of complex networks. For example, the contact processes [21] on annealed networks [22], for which the QS probability distribution at the transition point has the analytically known form [6]

$$\bar{P}(n) = \frac{1}{\sqrt{\Omega}} f\left(\frac{N}{\sqrt{\Omega}}\right), \quad (2)$$

where $\Omega = N/g$, $g = \langle k^2 \rangle / \langle k \rangle^2$ and $f(x)$ is a scaling function independent of the degree distribution. It is easy to show that $\langle n^l \rangle \sim \sqrt{\Omega}^l$, leading to $\chi \sim \sqrt{\Omega}$ and $\tilde{\chi} \sim \Omega/N \sim g^{-1}$. Using the scaling properties of g [23],

$$g \sim \begin{cases} k_c^{3-\gamma} \sim N^{(3-\gamma)/\omega} & 2 < \gamma < 3 \\ \text{const.} & \gamma > 3 \end{cases}, \quad (3)$$

for cutoff scaling as $k_c \sim N^{1/\omega}$, one concludes that, at $\lambda = \lambda_c$, $\chi \sim N^\vartheta$ and $\tilde{\chi} \sim N^{\vartheta'}$ where $\vartheta = \min[(\gamma - 3 + \omega)/2\omega, 1/2] > 0$ and $\vartheta' = \min[(\gamma - 3)/\omega, 0] \leq 0$. So, the susceptibility χ always diverges at the transition point while $\tilde{\chi}$ does not.

It is expected that the QS state does not depend on the initial condition. Figure 1 shows a comparison of QS simulations for the same network with different initial

densities $\rho(0) = 10^{-3}$ to 0.50. As can be seen, the results are completely independent of the initial condition. Also, the QS method was compared with the so-called ϵ -SIS model [24] where a small rate ϵ of spontaneous infection is assumed for each network vertex [25]. The thresholds involving long-term epidemics are the same as those of the QS method.

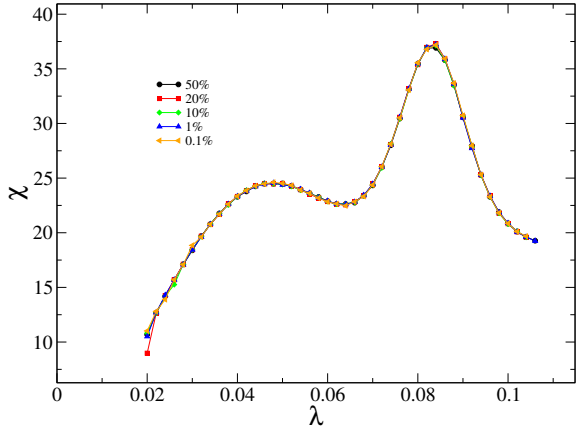


FIG. 1. Susceptibility against infection rate for SIS model with different fraction of initially infected vertices. The network parameters are $\gamma = 3.5$, $k_0 = 3$ and $N = 10^6$.

Reference [10] claimed, without a justification, that the QS method is unreliable for networks with degree exponents $\gamma > 3$ and proposed a new simulation strategy, which is referred here as lifespan method. We performed simulations of the SIS model using both methods. The lifespan method was implemented exactly as in Ref. [10]: The simulation starts with a single infected vertex and stops either the system visits the absorbing state or 50% of all vertices (the epidemic coverage) were infected at least once along the simulation. The duration of the simulation is computed and only runs that visited the absorbing state are used to compute the average lifespan since those that reached 50% of coverage are assumed as having an infinite lifespan. However such a criticism does not proceed. In fact, we verified that the lifespan method predict an epidemic threshold when the absorbing state becomes globally unstable, representing a long-term activity, but not necessarily the endemic phase. On other hand, the susceptibility analysis is able to simultaneously determine endemic as well as localized states (see examples discussed in Appendix A). So, we conclude that lifespan method must not be used in systems with multiple phase transitions since it is able to capture only one threshold.

III. NUMERICAL RESULTS

Two-peaks on susceptibility against infection rate for SIS were firstly reported in Ref. [9], which focused on the analysis of the peak at low λ and showed that it is

well described by the QMF theory (see also Ref. [14]) but did not realize that the peak at higher λ is the one associated to a diverging lifespan (Fig. 12 in appendix A). However, depending on the network realization, the susceptibility curves can exhibit much more complex behaviors with multiple peaks for values of λ larger than those reported in Refs. [9, 14]. These complex behaviors become very frequent for large networks. From now on we scrutinize such complex behavior to unveil its origin and implications to the epidemic activity.

Figure 2(a) shows a typical susceptibility curve (black) exhibiting such a complex behavior for a network generated with the configuration model [26], where vertex degree is selected from power-law distribution with a lower bound $k_0 = 3$ but without a predetermined upper cutoff. The degree distribution is shown in Fig. 2(d). Multiple peaks are observed whenever the degree distribution exhibits large gaps, in particular in the tails. These few vertices with degree $k \gg \langle k_{max} \rangle$, where k_{max} is the maximum value obtained in the generation of N random variables with distribution $P(k)$, are called outliers. Notice that these multiple peaks are not detected by the lifespan method [10]. The role played by outliers is evidenced by their immunizations [27] as illustrated in Fig. 2. For instance, the immunization of three most connected vertices is enough to destroy two peaks and to enhance others. Notice that the stationary density varies abruptly close to the thresholds determined via susceptibility peaks, Figs. 2(b) and (c), which is an evidence of the singular behavior of order parameter ρ .

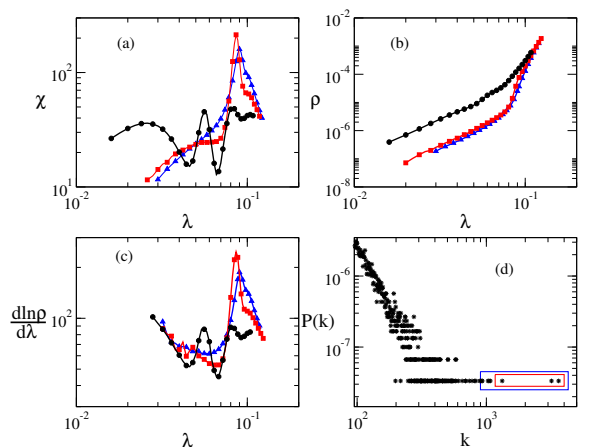


FIG. 2. (a) Susceptibility, (b) stationary density and (c) its logarithmic derivative versus infection rate for a SF networks with 3×10^7 vertices, degree exponent $\gamma = 3.5$, minimum degree $k_0 = 3$ and k_{max} unconstrained. The degree distribution is shown in panel (d). Different immunization strategies are shown: Black circles represents no immunization; red squares represent the immunization of three largest outliers (inner box in panel (d)); blue triangles represent the immunization of eight most connected vertices (outer box in panel (d)).

A deeper physical explanation for the multiple peaks can be obtained using an other order parameter, the par-

ticipation ratio (PR), which is defined as

$$\Phi = \frac{1}{N} \frac{(\sum_i \rho_i)^2}{\sum_i \rho_i^2}, \quad (4)$$

where ρ_i is the probability that the vertex i is infected in the stationary state. The inverse of the PR is a standard measure for localization/delocalization of states in condensed matter [28] and has been applied to statistical physics problems [29] including epidemic spreading on networks [8, 30]. The limiting cases of totally delocalized ($\rho_i = \rho \forall i$) and localized ($\rho_i = \rho \delta_{i,0}$ where 0 is the vertex where localization occurs) states are $\Phi = 1$ and $\Phi = 1/N$, respectively.

The PR as a function of the infection rate is shown in Fig. 3. The PR is an estimate of the fraction of vertices that effectively contributes to the epidemic activity. Thus, the multiple transitions are related to the rapid delocalization processes of the epidemics as λ increases, hallmarked by the singular behavior of Φ around distinct values of λ . When the PR corresponds to a finite fraction of the network in an active phase one has an authentic endemic state.

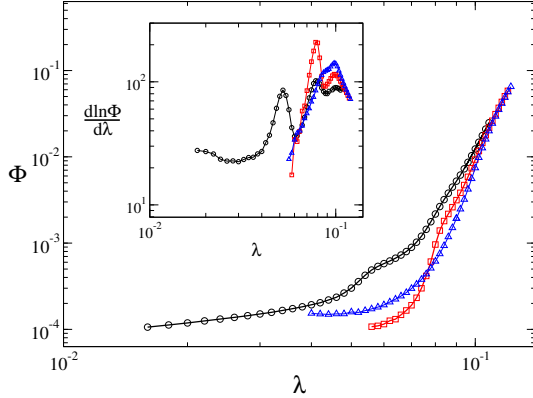


FIG. 3. Main: PR as a function of the infection rate for the same networks and immunization strategies shown in Fig. 2. Symbols as in Fig. 2. Inset: Logarithmic derivative of the PR as a function of the infection rate.

The logarithmic derivative of the PR exhibits several peaks in analogy to susceptibility peaks, as shown in the inset of Fig. 3. Indeed, PR can be seen as a susceptibility but from a origin different of χ . The latter is a measure of stochastic fluctuations of the order parameter (density of infected vertices) whereas the former is measure of stationary spatial fluctuations that make sense only for heterogeneous substrates.

The PR against network size for a fixed distance to either λ_p^{ls} (the threshold marking the lifespan divergence) and λ_p^{right} (the thresholds referent to the rightmost peak observed for susceptibility) are shown in Fig. 4(a). In the presented size range, the PR decays consistently with N^{-1} . Analogous results are obtained for $\bar{\rho}$ vs N curves (see Fig. 4(b)). These decays constitute a proof for epidemics localization at $\lambda \gtrsim \lambda_p^{ls}$ whereas the constant de-

pendence on N observed for $\lambda \gtrsim \lambda_p^{right}$ represents an endemic phase [31].

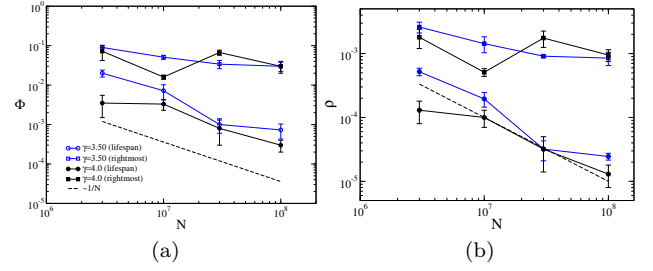


FIG. 4. (a) . (a) PR against size for a fixed distance to either λ_p^{ls} or λ_p^{right} . (b) Density against size for a fixed distance $\lambda - \lambda_p = 0.012$ to either lifespan and rightmost peaks. Networks are the same used in Fig. 3.

Figure 5 shows the positions λ_p^{left} (the thresholds referent to the leftmost peak in the susceptibility curves) as well as λ_p^{right} and λ_p^{ls} against the network size. One can see that λ_p^{right} is constant for large N whereas the other ones neatly decays with N . Our results show that the case $\gamma > 3$ may concomitantly show phases transitions predicted by three competing mean-field theories: (i) At $\lambda = \lambda_p^{left}$, one has a transition to a short-term epidemics highly concentrated at the most connected vertex and its neighborhood. The threshold dependence on size is very well described by QMF theories [7, 9, 14]. (ii) At $\lambda = \lambda_p^{ls}$, a transition to a long-term epidemics with a threshold described by the BCPS theory [10] is observed but it is not endemic since PR and ρ decay with N even quite above this threshold. Notice that the threshold λ_p^{ls} decays much slower than λ_p^{left} . (iii) For $\lambda = \lambda_p^{right}$, a transition involving an authentic endemic phase with a finite threshold is observed as formerly, and now surprisingly, predicted by the HMF theory [3].

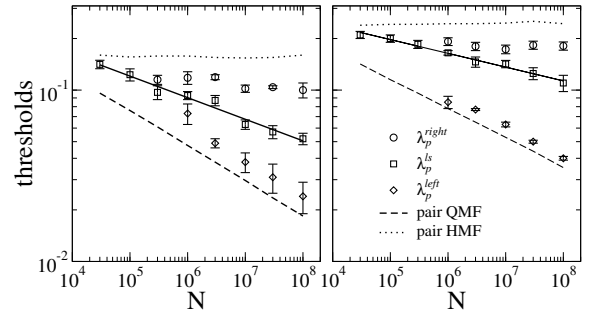


FIG. 5. Thresholds for SIS dynamics on SF networks with degree exponents $\gamma = 3.5$ (left) and $\gamma = 4.0$ (right). Averages were done over 3 network realizations. The results predicted by pair QMF [14] and pair HMF [6] theories are shown as dashed and dotted lines, respectively. Solid lines are power law regressions.

The co-existence of localized and endemic phase transitions in a same network can be explained in a double random regular network (DRRN), Fig. 6. These networks

are formed by two random regular networks (RRNs) [9], of sizes N_1 and $N_2 = N_1^\alpha$ ($\alpha < 1 \Rightarrow N_2/N_1 \rightarrow 0$ in the thermodynamical limit) and degree m_1 and m_2 , respectively, connected by a single edge. This network has two epidemic thresholds corresponding to the activations of single RRNs. Choosing $m_1 = 6$ and $m_2 = 4$, the thresholds determined for single RRNs are $\lambda_c^{(1)} = 0.31452$ ($m_1 = 4$, present work) and $\lambda_c^{(2)} = 0.2026$ ($m_2 = 6$ [20]). By construction, the former involves an endemic and latter a localized phase transition since the smaller RRN constitutes itself a vanishing fraction of the whole network. Figure 6 shows the susceptibility plots for $\alpha = 0.5$ with peaks converging exactly to the expected thresholds. The threshold obtained via lifespan method, which is in principle fitted by the BCPS theory, converges to the no localized one (see appendix A for additional data and discussions). Notice that this network model can be generalized to produce an arbitrary number of phase transitions.

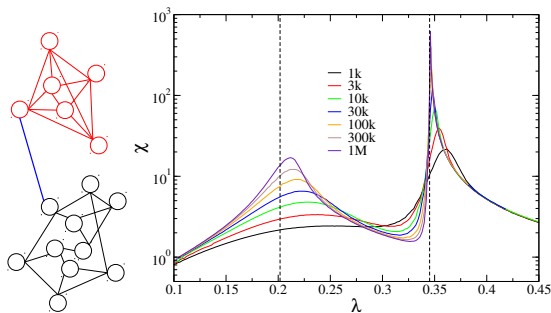


FIG. 6. Left: Schematics of a double random regular network (DRRN). Right: Susceptibility against infection rate for DRRNs with using $m_1 = 4$, $m_2 = 6$, $\alpha = 1/2$ and different sizes. Dashed lines are thresholds predicted for DRRNs.

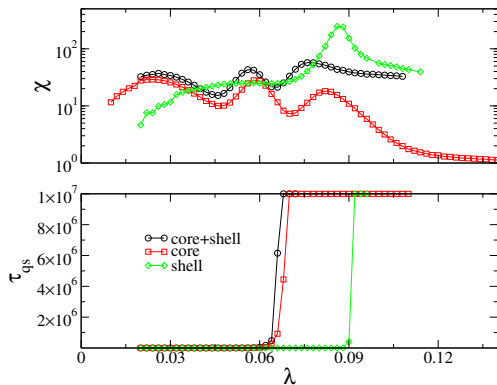


FIG. 7. Susceptibility (top) and QS lifespan (bottom) against infection rate for SIS dynamics on a network with $N = 3 \times 10^7$ and degree exponent $\gamma = 3.50$ restricted to different domains. The lifespan is considered infinite if greater than the averaging time $t_{av} = 10^7$.

We have now a simple physical explanation for multiple thresholds observed in SF networks with $\gamma > 3$: Most connected vertices are frequently nearest neighbors

(NNs) forming a densely connected core containing a few vertices. The subset containing this core plus its NNs forms a subgraph with $N_2 \sim \sum_{k > \langle k_{max} \rangle} NP(k)k \sim N^{1/(\gamma-1)} \ll N$. The domain size diverges as network size increases, and is able to sustain a stable epidemic activity, but still represents a vanishing fraction of the whole the network. Above the activation of this domain but still below the endemic phase, the epidemics is eventually transmitted to the any other vertex of the network due to the small-world property, but this activity dies out since the process is locally sub-critical. However, all network vertices will be infected for a while since the active central core acts as a constant source of infectiousness to the rest of the network.

Our conjecture is confirmed in Fig. 7 where SIS dynamics in a large network ($N = 3 \times 10^7$ vertices) is compared with dynamics restricted to either its core of outliers (7 most connected vertices) plus their NNs (≈ 13200 vertices) or to its outer shell excluding the densely connected core [32]. The multiple peaks for the core are observed approximately at same place as those for the whole network but the outer shell exhibits a single peak coinciding with λ_p^{right} . However, the lifespan determined via QS method (see appendix A) diverges at $\lambda \approx \lambda_c^{ls}$ for both core and whole network whereas the divergence coincides with λ_p^{right} for the outer shell.

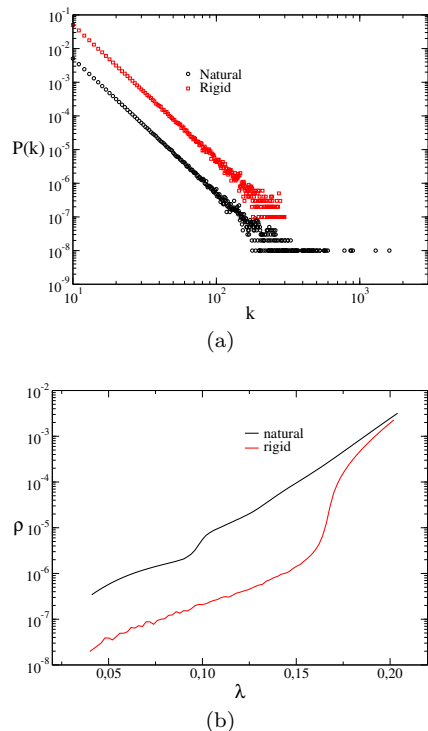


FIG. 8. Analysis of SIS model on networks with natural and rigid cutoffs. (a) The tail of the degree distributions for $\gamma = 4$ with $N = 10^8$ vertices. The rigid cutoff curve was shifted to enhance visibility. (b) QS density against infection rate for a network degree exponent $\gamma = 4.0$ using different cutoffs

Notice that outliers play an important role even not being able to produce alone an endemic phase. In order to highlight their effects, we investigated networks with a rigid cutoff $k_{max} = k_0 N^{0.75/(\gamma-1)}$, which suppresses emergence of outliers in networks. Networks without an rigid upper bound in the degree distribution have a highly fluctuating natural cutoff with an average value $\langle k_{max} \rangle \simeq k_0 N^{1/(\gamma-1)}$ [23]. We introduce a hard cutoff as $k_{max} = k_0 N^{0.75/(\gamma-1)}$, which suppresses emergence of outliers, Fig. 8(a). Fig. 8(b) shows the QS density for rigid and natural cutoffs. The infectiousness for $\lambda < \lambda_c^{endemic}$ is highly reduced in the absence of outliers. The susceptibility no longer exhibit multiple peaks for a hard cutoff, Fig. 9(a), confirming the existence of a single phase transition. Also, the hard cutoff thresholds are quite close to λ_p^{right} obtained for the natural cutoff, as shown in Fig. 9(b). Such an observation is in agreement with the HMF theory where the thresholds for $\gamma > 3$ are asymptotically independent of how k_c diverges [3, 6]. Also, the infectiousness below the endemic threshold is highly reduced in the absence of outliers, attesting their importance for the epidemic activity.

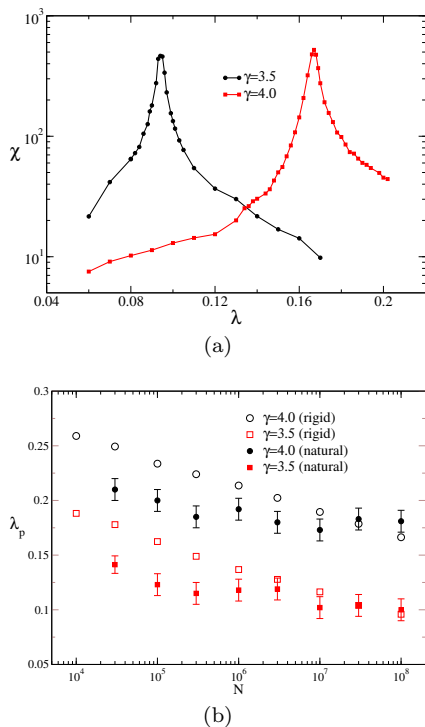


FIG. 9. The SIS model on networks with natural and rigid cutoffs. (a) Susceptibility curves for networks with rigid cutoff, $N = 10^8$ vertices and different degree exponent. (b) Threshold against system size for rigid and natural cutoffs. Averages were done over three networks and error bars for rigid cutoff are smaller than symbols.

IV. CONCLUSIONS

In summary, we thoroughly simulated the dynamics of the SIS epidemic model on complex networks with power law degree distributions with exponent $\gamma > 3$, for which conflicting theories discussing the existence or not of a finite epidemic threshold for the endemic phase have recently been proposed [7, 8, 10, 11]. We show that the SIS dynamics can indeed exhibit several phase transitions associated to different epidemiological scenarios and the one associated to the transition to an endemic state, in which a finite fraction of network is infected, occurs at a finite threshold as formerly and now surprisingly foreseen by the HMF theory [3]. We also show that the threshold obtained recently in the BCPS mean-field theory [10] represents a transition to a long-term but still localized epidemics. The multiple phase transitions are associated to large gaps in the degree distribution.

Our finds are partially consistent with the conjecture proposed by Lee *et al.* [11] since the lifespans of independent domains involving a set of outliers grow exponentially fast with their sizes implying that long-term states are sustainable even in non-endemic phase. Our results also do not rule out the mean-field analysis of Ref. [8]. The intermediary transitions can be associated to distinct localized eigenvectors that are centered on the outliers while the endemic threshold involves a delocalized eigenvector with a finite eigenvalue.

Apparently competing mean-field theories [3, 7, 8, 10, 11] are, in fact, complementary and describe distinct transitions that may concomitantly appear depending on the network structure. In particular, the transitions involving localized phases, as the one predicted by the BCPS theory [10], are not necessarily negligible since they become long-term and an epidemic outbreak may eventually reach a finite fraction of the network. This peculiar result is unthinkable for other substrates rather than complex networks sharing the small-world and scale-free properties. Actually, it is well known that some computer viruses can survive for long periods (years) in a very low density (below 10^{-4}) [33] exemplifying the importance of metastable non-endemic states. Our numerical results call for general theoretical approaches to describe in a unified framework the multiple phase transitions of the SIS dynamics.

ACKNOWLEDGMENTS

This work was partially supported by the Brazilian agencies CAPES, CNPq and FAPEMIG. Authors thank Romualdo Pastor-Satorras and Claudio Castellano for the critical and profitable discussions and Ronald Dickman for priceless suggestions.

Appendix A: Quasistationary versus lifespan methods

Lets start showing that the QS methods succeeds whereas lifespan method fails in predicting the endemic phase for a double random regular network (DRRN) (Fig. 4). In a single RRN all vertices have the same degree m but connections are done at random avoiding multiple and self connections [9]. The thresholds are finite and slightly above $\lambda_c = 1/(m-1)$ given by a pair approximation [9, 14]. In the case of a DRRN with degrees m_1 and m_2 ($m_1 < m_2$) for each sub-graph of sizes N_1 and N_2 , respectively, one expects two phase transitions, corresponding to the activations of each domain, with thresholds approximately given by $\lambda_c^{(i)} \gtrsim 1/(m_i - 1)$

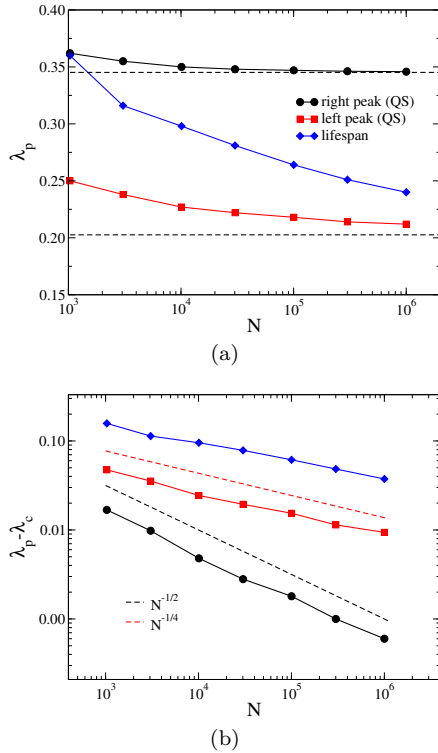


FIG. 10. (a) The thresholds estimated as the peaks in the susceptibility or lifespan curves. The dashed lines are thresholds obtained on single RRNs with the respective m_i . (b) Difference between peaks and the thresholds for single RRNs with $m = 4$ (lifespan and left susceptibility peaks) or $m = 6$ (right susceptibility peak).

The susceptibility peaks in Fig. 6 clearly converge to the repective thresholds of single RRNs as shown in Fig. 10(a) and (b). Notice that the mean-field theory for the finite size scaling of the contact process, which, in the case of stricly homogeneous networks, is exactly the same as SIS model with an infection rate λ/m predicts that the threshold approaches its asymptotic values as $\lambda_p - \lambda_c \sim S^{-1/2}$, where S is the network size [6]. So, the endemic threshold is expected to scale

as $\lambda_p - \lambda_c^{(1)} \sim N_1^{-1/2} \sim N^{-1/2}$ and the localized one as $\lambda_p - \lambda_c^{(2)} \sim N_2^{-1/2} \sim N^{-\alpha/2}$. These power-laws are confirmed in Fig. 10(b). The lifespan curves have single peaks that converge to the threshold corresponding to a localized epidemic and interestingly following the same scaling law as the QS peak as shown in Figs 10 and Fig. 11. The central point here is that the lifespan method detects the first threshold where the absorbing state becomes globally unstable (a long-term activity) which is not necessarily the endemic one. It is worth noticing that the QS simulations around the peaks are orders of magnitude computationally more efficient than the lifespan ones.

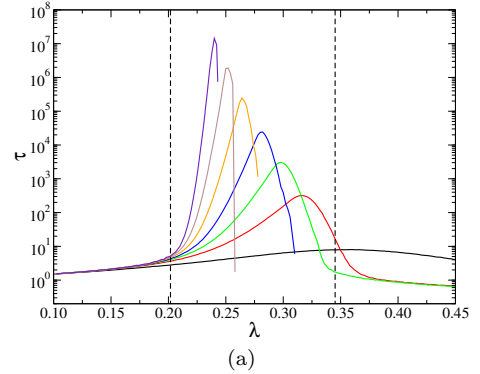


FIG. 11. The lifespan against creation ratio for SIS model on DRRNs with $m_1 = 4$ and $m_2 = 6$, $N_2 = \sqrt{N_1}$, and $N_1 = 10^3, 3 \times 10^3, 10^4, 3 \times 10^4, 10^5, 3 \times 10^5, 10^6$ increasing from the right.

We also performed simulations of the SIS model on networks generated by the uncorrelated configuration (UCM) model [26] with $\gamma = 3.50$, minimum degree $k_0 = 3$, and upper cutoff $k_{max} = \langle k_{max} \rangle$, to compare with the results of Ref. [10], which casted doubt on the validity of the QS method for this type of the network. The constraint $k_{max} = \langle k_{max} \rangle$ avoids fluctuations in the most connected vertex and, consequently, in the largest eigenvalue of the adjacency matrix and is useful for comparisons with the QMF theory [9]. We remark that the constraint $k_{max} = \langle k_{max} \rangle$ is just used in this appendix.

Figures 12(a) and (b) show the lifespan and susceptibility against infection rate for networks of different sizes. The peak positions against network size are compared in Fig 12(c). As can be clearly seen, the right susceptibility peaks are very close to the lifespan ones showing that the susceptibility method is able to capture the same transitions as the lifespan method does but going beyond as discussed in the main text. Moreover, a diverging characteristic time is also obtained in the QS method since the QS lifespan is given by $\tau = 1/P(1)$ [16].

We have checked that the lifespans obtained in the QS method and those of Ref. [10] diverge at the same threshold. It is worth noticing that if larger values of λ are simulated, other peaks will emerge in susceptibility curves even using the cutoff $k \leq \langle k_{max} \rangle$. This fact

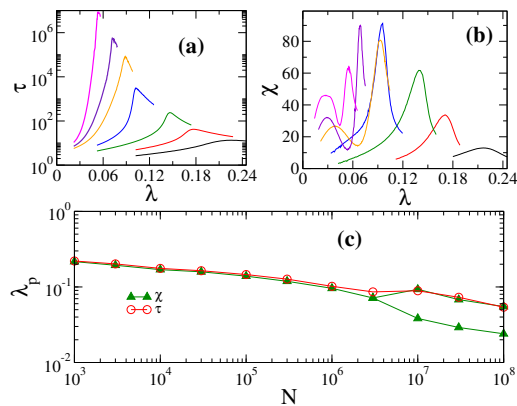


FIG. 12. Numerical determination of the thresholds for the SIS model on UCM networks with $\gamma = 3.50$, $k_0 = 3$ and $k_{max} = \langle k_{max} \rangle$ for network sizes $N = 10^3, 10^4, 10^5, 10^6, 10^7, 3 \times 10^7, 10^8$ increasing from the right. Both (a) lifespan and (b) susceptibility methods are shown in the top panels. (c) Peak positions as functions of the network size estimated with both methods.

was not noted in previous works dealing with this same network model [9, 10, 14].

-
- [1] S. N. Dorogovtsev, A. V. Goltsev, and J. F. F. Mendes, Rev. Mod. Phys. **80**, 1275 (2008).
 - [2] R. Albert, H. Jeong, and A.-L. Barabási, Nature **406**, 378 (2000).
 - [3] R. Pastor-Satorras and A. Vespignani, Phys. Rev. Lett. **86**, 3200 (2001); Phys. Rev. E **63**, 066117 (2001).
 - [4] S. N. Dorogovtsev, A. V. Goltsev, and J. F. F. Mendes, Phys. Rev. E **66**, 016104 (2002).
 - [5] M. Henkel, H. Hinrichsen, S. Lübeck, and M. Pleimling, *Non-equilibrium phase transitions*, Vol. 1 (Springer, Dordrecht, Netherlands, 2008).
 - [6] C. Castellano and R. Pastor-Satorras, Phys. Rev. Lett. **100**, 148701 (2008); H. Hong, M. Ha, and H. Park, **98**, 258701 (2007); R. Juhász, G. Ódor, C. Castellano, and M. A. Muñoz, Phys. Rev. E **85**, 066125 (2012); A. S. Mata, R. S. Ferreira, and S. C. Ferreira, N. J. Phys. **16**, 053006 (2014); S. C. Ferreira, R. S. Ferreira, and R. Pastor-Satorras, Phys. Rev. E **83**, 066113 (2011).
 - [7] C. Castellano and R. Pastor-Satorras, Phys. Rev. Lett. **105**, 218701 (2010).
 - [8] A. V. Goltsev, S. N. Dorogovtsev, J. G. Oliveira, and J. F. F. Mendes, Phys. Rev. Lett. **109**, 128702 (2012).
 - [9] S. C. Ferreira, C. Castellano, and R. Pastor-Satorras, Phys. Rev. E **86**, 041125 (2012).
 - [10] M. Boguñá, C. Castellano, and R. Pastor-Satorras, Phys. Rev. Lett. **111**, 068701 (2013).
 - [11] H. K. Lee, P.-S. Shim, and J. D. Noh, Phys. Rev. E **87**, 062812 (2013).
 - [12] E. Cator and P. Van Mieghem, Phys. Rev. E **85**, 056111 (2012); P. V. Mieghem, Eur. Lett. **97**, 48004 (2012).
 - [13] D. Chakrabarti, Y. Wang, C. Wang, J. Leskovec, and C. Faloutsos, ACM Trans. Inf. Syst. Secur. **10**, 1 (2008).
 - [14] A. S. Mata and S. C. Ferreira, Eur. Lett. **103**, 48003 (2013).
 - [15] H. K. Lee, P.-S. Shim, and J. D. Noh, Preprint, ArXiv:1309.5367 (2013); M. Boguñá, C. Castellano, and R. Pastor-Satorras, preprint arXiv:1403.7913 (2014).
 - [16] M. M. de Oliveira and R. Dickman, Phys. Rev. E **71**, 016129 (2005).
 - [17] S. C. Ferreira, R. S. Ferreira, and R. Pastor-Satorras, Phys. Rev. E **83**, 066113 (2011).
 - [18] M. Newman, *Networks: An Introduction* (Oxford University Press, Inc., New York, NY, USA, 2010).
 - [19] D. J. Watts and S. H. Strogatz, nature **393**, 440 (1998).
 - [20] R. S. Ferreira and S. C. Ferreira, Eur. Phys. J. B **86**, 1 (2013).
 - [21] J. Marro and R. Dickman, *Nonequilibrium phase transitions in lattice models* (Cambridge University Press, Cambridge, 1999).
 - [22] In annealed networks, the vertex degrees are fixed while the edges are completely rewired between successive dynamics steps implying that dynamical correlations are absent and HMF theory becomes an exact prescription [1].
 - [23] M. Boguñá, R. Pastor-Satorras, and A. Vespignani, Eur. Phys. J. B **38**, 205 (2004).
 - [24] P. Van Mieghem and E. Cator, Phys. Rev. E **86**, 016116 (2012).
 - [25] R. S. Sander and S. C. Ferreira, in preparation.
 - [26] M. Catanzaro, M. Boguñá, and R. Pastor-Satorras, Phys. Rev. E **71**, 027103 (2005).
 - [27] Immunized vertices cannot be infected, which is equivalent to remove them from the network.
 - [28] R. J. Bell and P. Dean, Discuss. Faraday Soc. **50**, 55 (1970).
 - [29] V. Plerou, P. Gopikrishnan, B. Rosenow, L. A. Nunes Amaral, and H. E. Stanley, Phys. Rev. Lett. **83**, 1471 (1999).
 - [30] M. Barthélemy, A. Barrat, R. Pastor-Satorras, and A. Vespignani, Phys. Rev. Lett. **92**, 178701 (2004); G. Ódor, Phys. Rev. E **88**, 032109 (2013).
 - [31] Notice that a scaling $\bar{\rho} \sim (\lambda - \lambda_p)^\beta$, independent of the size, is expected for a usual endemic phase transition in the thermodynamic limit [5]. On other hand, a constant

PR implies that a non-vanishing fraction of the networks effectively contribute for sustaining epidemics.

- [32] To restrict the epidemics to the core we immunize the shell and vice-versa.

- [33] R. Pastor-Satorras and A. Vespignani, *Evolution and structure of the Internet: A statistical physics approach* (Cambridge University Press, Cambridge, 2004).